



## A study in thermoelectric effect of $\text{Eu}_2\text{O}_3$ substitution on $\text{Al}_2\text{O}_3$ in $\text{CuAl}_{(100-x)}\text{Eu}_{(x)}\text{O}_2$

Kitipun Boonin<sup>a, b, \*</sup>, Peerapong Yamchumporn<sup>a, b</sup>, Kunchit Singsoog<sup>c</sup>, Jakrapong Kaewkhaao<sup>a, b</sup>

<sup>a</sup> Physics Program, Faculty of Science and Technology, Nakhon Pathom Rajabhat University, Meuang, Nakhon Pathom, 73000 Thailand

<sup>b</sup> Center of Excellence in Glass Technology and Materials Science, Nakhon Pathom Rajabhat University, Meuang, Nakhon Pathom, 73000 Thailand

<sup>c</sup> Thermoelectric Research Laboratory, Center of Excellence on Alternative Energy, Research and Development Institution, Sakon Nakhon Rajabhat University, Sakon Nakhon, 47000 Thailand

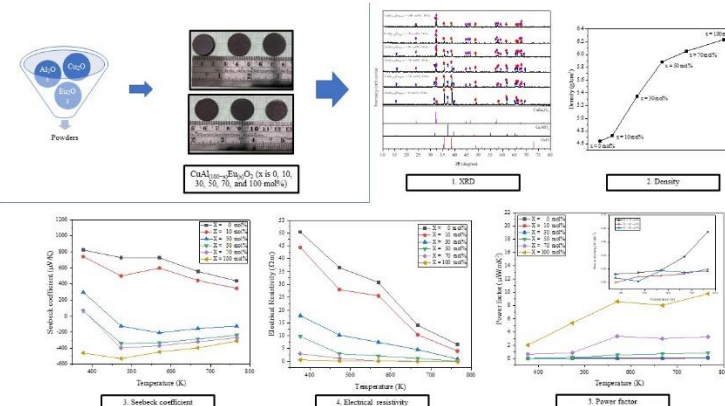
\*Corresponding Author: kbcegm@gmail.com

<https://doi.org/10.55674/jmsae.v11i3.251500>

Received: 29 January 2023 | Revised: 10 February 2023 | Accepted: 19 July 2023 | Available online: 1 September 2023

### Abstract

The effects of  $\text{Eu}_2\text{O}_3$  substitution on  $\text{Al}_2\text{O}_3$  in  $\text{CuAl}_{(100-x)}\text{Eu}_{(x)}\text{O}_2$  ( $x = 0, 10, 30, 50, 70$ , and  $100$  mol%) were considered. In this study, all samples with a diameter of 20 mm were sintered by using solid-state reaction method. The structural analysis with XRD investigation shows that it had a hexagonal  $\text{CuAlO}_2$  structure at  $x = 0, 10, 30$ , and  $50$  mol%. Tetragonal  $\text{CuEu}_2\text{O}_4$  structures were reported at  $x = 10, 30, 50, 70$ , and  $100$  mol%. The ZEM-3 instrument measures thermoelectric characteristics like the Seebeck coefficient, electrical resistivity, and power factor throughout the temperature range of  $350 - 800$  K. According to the investigation, the electrical resistivity value tended to continue to decrease as measurement temperature increased. The Seebeck coefficient shows a positive value. However, when  $\text{Al}_2\text{O}_3$  was substituted for  $\text{Eu}_2\text{O}_3$  in large amounts, the Seebeck coefficient value became negative. The power factor increases as the mole ratio of  $\text{Eu}_2\text{O}_3$  increase, exhibited the highest value of around  $9.50 \mu\text{W mK}^{-2}$  at  $775$  K.



**Keywords:** Solid-state reaction; Seebeck coefficient; Power factor

© 2023 Center of Excellence on Alternative Energy reserved

### Introduction

Because waste heat can be converted to electrical energy, the development of thermoelectric materials is critical for convert energy. Improved thermoelectric material performance is a crucial factor to take into account. The performance of thermoelectric materials can be identified using a parameter called the figure of merit,  $Z = \sigma\alpha^2/\kappa$ , where  $\sigma$ ,  $\alpha$ , and  $\kappa$  are the electrical conductivity, Seebeck coefficient, and thermal conductivity, respectively [1]. Large values of  $Z$  are indicators of good thermoelectric material performance, and it is important to get high  $\sigma$ , high  $\alpha$ , and low  $\kappa$  values.

For industries that work in high temperature situations some thermoelectric materials, such as SnSe [2, 3], PbTe [4, 5], and Bi-Te [6, 7] have performance limitations as a result of this. At a temperature of 300 K, I. Terasaki et al. reported a  $\text{NaCo}_2\text{O}_4$  thermoelectric material with a high  $Z$  value of  $8.8 \times 10^{-4}$  and a big  $S$  of  $100 \mu\text{V K}^{-1}$  [8]. The usage of  $\text{NaCo}_2\text{O}_4$  is nonetheless constrained by sodium's inability to withstand temperatures higher than 1073 K and by air humidity [9]. As a result, high-performance and environmentally stable new oxide materials must be created. Creating novel oxide materials remains the most critical

challenge for practical thermoelectric power-generating applications [10-11]. CuAlO<sub>2</sub> compounds, particularly illustrate excellent performance for thermoelectric materials that operate at high temperatures. At high temperatures, Park et al. [12] and Liu et al. [13] found that the temperature independence of CuAlO<sub>2</sub> thermoelectric characteristics for Seebeck coefficient, thermal conductivity, power factor, and ZT is about 5  $\mu$ V K<sup>-1</sup>, 0.20 W cmK<sup>-1</sup>,  $4 \times 10^{-5}$  W mK<sup>-2</sup>, and 0.0045, respectively. Chattopadhyay et al. [14] were investigated the thermoelectric and electrical characteristics of CuAlO<sub>2</sub> thin films produced with dc-sputtering. It is generally established that altering the microstructure and carrier concentration by substitution is a suitable technique of improving thermoelectric performance.

The thermoelectric characteristics of Eu<sub>2</sub>O<sub>3</sub> substitution on Al<sub>2</sub>O<sub>3</sub> in CuAl<sub>(100-x)</sub>Eu<sub>(x)</sub>O<sub>2</sub> (x = 0, 10, 30, 50, 70, and 100 mol%) pellet of ceramics with a diameter of 20 mm synthesized by the solid-state reaction process are investigated. The thermoelectric properties of the samples: electrical resistivity, Seebeck coefficient, and power factor were investigated by ZEM-3. The results of this study are likely to assist in the optimization of thermoelectric materials CuAlO<sub>2</sub>.

## Materials and Methods

When x is 0, 10, 30, 50, 70, and 100 mol%, we should calculate using the stoichiometry method in the chemical formula CuAl<sub>(100-x)</sub>Eu<sub>(x)</sub>O<sub>2</sub>. Cu<sub>2</sub>O with a purity of 99.99%, Al<sub>2</sub>O<sub>3</sub> with a purity of 99.99%, and Eu<sub>2</sub>O<sub>3</sub> with a purity of 99.99% were utilized in this method for the calculated post-material synthesis. This work synthesized the material in an electric furnace by a solid-state reaction method. The powder of the chemical mixture was calcined at 373 K for 2 hr to remove organic matter and moisture. The calcined powder was ball milled for 3 hr at 200 rpm with agate balls as the grinding medium. The dry powder was pressed using a hand press at a pressure of 300 MPa to prepare 20 mm diameter pellets. All pellets were sintered inside a furnace at 1173 K for 10 hr in air, and then the furnace was cooled down to room temperature.

X-ray diffraction was used to determine the samples' phases (XRD; Shimadzu XRD-6100) with CuK $\alpha$  radiation accelerated in a 2 $\theta$  range of 10 – 80 degrees. The Archimedes principle of density (A&D HR-200) was used to confirm the physical characteristics. The Seebeck coefficient, electrical resistivity, and power factor were measured (ZEM-3; Ulvac, Inc.) in the temperature range 350 – 800 K.

## Results and Discussions

All of X-ray diffraction patterns of CuAl<sub>(100-x)</sub>Eu<sub>(x)</sub>O<sub>2</sub> (x is 0, 10, 30, 50, 70, and 100 mol%) samples follow the molar ratio of Eu<sub>2</sub>O<sub>3</sub> from 0 until 1 by mol% were shown in Fig. 1. These results presented the primary phase in CuO (Monoclinic, JCPDS No.00-048-1548) for all samples. CuAlO<sub>2</sub> (Hexagonal, JCPDS No.00-040-1037) for samples with increased Eu<sub>2</sub>O<sub>3</sub> of 0.1, 0.3, and 0.5 mol % and CuEu<sub>2</sub>O<sub>4</sub> (Tetragonal, JCPDS No.00-052-1719) for all samples except those without Eu<sub>2</sub>O<sub>3</sub>. The amplitude of the CuEu<sub>2</sub>O<sub>4</sub> peak was observed to increase as the Eu<sub>2</sub>O<sub>3</sub> concentration increased. Throughout the 350 K to 800 K temperature range, the ZEM-3 was utilized to measure thermoelectric properties.

In Fig. 2, the density is shown on the y-axis as the Eu<sub>2</sub>O<sub>3</sub> content increases on the x-axis. The sample density measurement indicates the decreasing impact of Al<sub>2</sub>O<sub>3</sub> and the increasing amount of Eu<sub>2</sub>O<sub>3</sub> in the CuAlO<sub>2</sub> and CuEu<sub>2</sub>O<sub>4</sub> phases, and Eu<sub>2</sub>O<sub>3</sub> has a higher density than Al<sub>2</sub>O<sub>3</sub>. The increase in Eu<sub>2</sub>O<sub>3</sub> content inside the sample causes an increase in the density value. The material with the most excellent density was 6.24 g cm<sup>-3</sup> of Eu<sub>2</sub>O<sub>3</sub> in mol%.

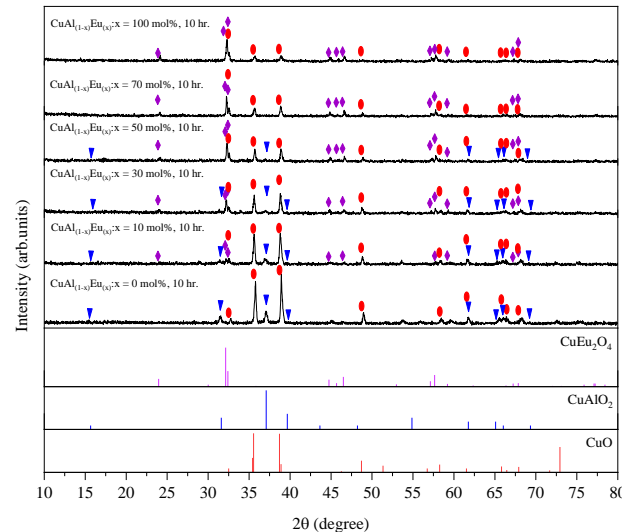


**Fig. 1** X-ray diffraction patterns of CuAl<sub>(100-x)</sub>Eu<sub>(x)</sub>O<sub>2</sub> (x is 0, 10, 30, 50, 70, and 100 mol%).

The Seebeck coefficient's sign, which is positive for the conductivity of holes and negative for the conductivity of electrons, reflects the electrical conductivity of the material under investigation. The Seebeck coefficients for all samples with increased Eu<sub>2</sub>O<sub>3</sub> from x = 0 to x = 100 mol% are shown in Fig. 3. The conductivity behavior of materials was changed from hole conductivity to electron conductivity [15]. The electrical conductivity of a system increases as the

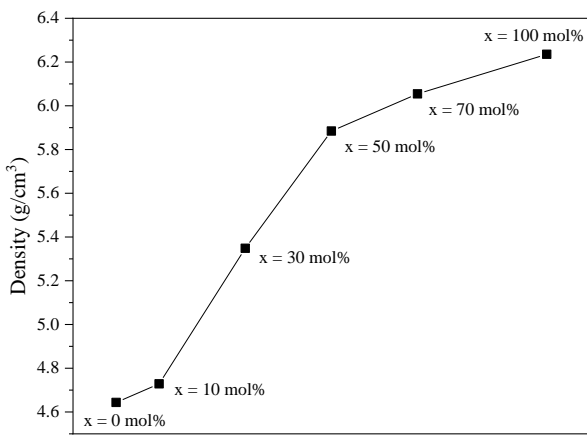


**Fig. 2** Density of  $\text{CuAl}_{(100-x)}\text{Eu}_{(x)}\text{O}_2$  ( $x$  is 0, 10, 30, 50, 70, and 100 mol%).

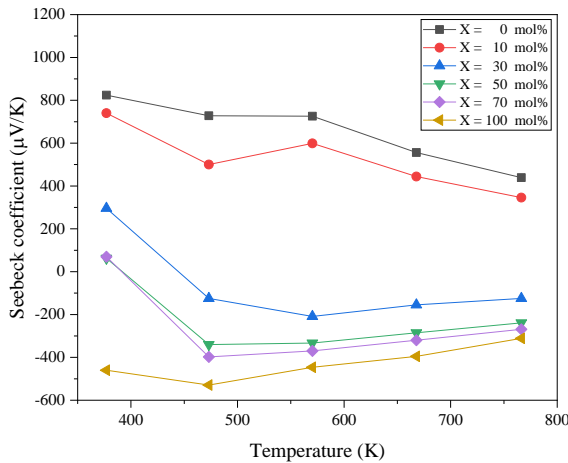


**Fig. 3** Temperature dependence on Seebeck coefficient of  $\text{CuAl}_{(100-x)}\text{Eu}_{(x)}\text{O}_2$  ( $x$  is 0, 10, 30, 50, 70, and 100 mol%).

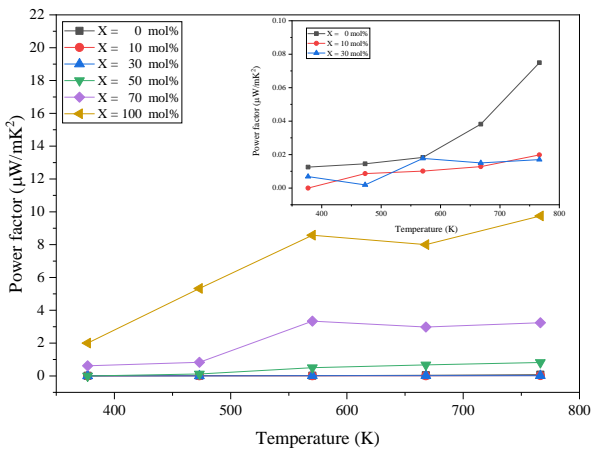


**Fig. 5** Temperature dependence on Power factor of  $\text{CuAl}_{(100-x)}\text{Eu}_{(x)}\text{O}_2$  ( $x$  is 0, 10, 30, 50, 70, and 100 mol%).

carrier density raises. The Seebeck coefficient in the measured sample was determined to be trending downward when the measurement temperature was raised. The sample where  $x$  is 0 mol% at 377 K has the highest value of  $824 \mu\text{V K}^{-1}$  for the measured Seebeck coefficient. The Mott relation can be used to explain the Seebeck coefficients tendency [16].

$$S(T) = \frac{\pi^2 k_B^2 T}{3e} \left[ \frac{N(E)}{n} + \left( \frac{\partial \ln \mu(E)}{\partial E} \right)_{E=E_F} \right] \quad (1)$$

where  $S$  are Seebeck coefficient ( $S$ ), the Boltzmann constant ( $k_B$ ), carrier concentration ( $n$ ), and density of state ( $N(E)$ ), respectively. Fig. 4 shows that when the molar ratio of  $\text{Eu}_2\text{O}_3$  rises, the electrical resistivity of  $\text{CuAl}_{(100-x)}\text{Eu}_{(x)}\text{O}_2$  samples decreases with increasing temperature throughout the whole temperature range. The electrical resistivity  $\rho$  and the Seebeck coefficient  $S$  were used to analyses the power factor  $P = S^2/\rho$ . Fig. 5 shows the power factor calculated from the data in Figure 3 and 4. With increasing temperature, the power factor of the  $\text{CuAl}_{(100-x)}\text{Eu}_{(x)}\text{O}_2$  samples tends to rise. The highest value of the sample is defined as  $9.75 \mu\text{W mK}^{-2}$  when  $x$  is 1 at 775 K after determining the power factor that tends to rise with increasing temperature utilized in the measurement as shown in Fig. 5. Based on the findings, it's thought that polycrystalline  $\text{CuAl}_{(100-x)}\text{Eu}_{(x)}\text{O}_2$  might be useful in high temperature thermoelectric applications.

## Conclusion

The main phase present in the sintered bulk samples of  $\text{CuAl}_{(100-x)}\text{Eu}_{(x)}\text{O}_2$  ( $0 \leq x \leq 1$ ) is Tetragonal structure, I4/mmm, combination with other phases such as  $\text{CuO}$  and  $\text{CuAlO}_2$ . With the ZEM-3 instrument, the measuring temperature range of 350 – 800 K was determined to assess the thermoelectric characteristics. The  $\text{CuAl}_{(100-x)}\text{Eu}_{(x)}\text{O}_2$  samples Seebeck coefficient reduced as the  $\text{Eu}_2\text{O}_3$  concentration increased, result of an increase in carrier density. The electrical resistivity decreases with increasing temperature throughout the whole temperature range. Because of a consider the effects in electrical conductivity, adding  $\text{Eu}_2\text{O}_3$  up to  $x = 100$  mol% resulted in a significant rise in power factor. The highest value of power factor  $9.75 \mu\text{W mK}^{-2}$  on  $x$  is 100 mol% of  $\text{Eu}_2\text{O}_3$  at 775 K. As a result, adding  $\text{Eu}_2\text{O}_3$  to  $\text{CuAlO}_2$  improved the thermoelectric properties of the material at high temperatures.

## Acknowledgement

This project is funded by National Research Council of Thailand (NRCT) and TENSOR PRODUCTS LIMITED PARTNERSHIP no. N41A650415. The authors would like

to thanks Thermoelectric Research Laboratory, Center of Excellence on Alternative Energy (CEAE), Research and Development Institution, Sakon Nakhon Rajabhat University for thermoelectric properties measurements, Thanks are also due to Research and Development Institute, NRU for facilities. K. Boonin and J. Kaewkha would like to thanks National Research Council of Thailand (NRCT) and Thailand Science Research and Innovation (TSRI) for supporting this research.

## References

- [1] [1] D.M. Rowe, CRC Handbook of Thermoelectrics, first ed., Boca Raton, New York, 1995.
- [2] L.D. Zhao, G. Tan, S. Hao, J. He, Y. Pei, H. Chi, H. Wang, S. Gong, H. Xu, V.P. Dravid, C. Uher, G.J. Snyder, C. Wolverton, M.G. Kanatzidis, Ultrahigh power factor and thermoelectric performance in hole-doped single-crystal SnSe, *Science*, 351 (2015) 1 – 7.
- [3] A.T. Duong, V.Q. Nguyen, G. Duvjir, V.T. Duong, S. Kwon, J.Y. Song, J.K. Lee, J.E. Lee, S. Park, T. Min, J. Lee, J. Kim, S. Cho, Achieving ZT=2.2 with Bi-doped n-type SnSe single crystals, *Nature Com.* 7 (2016) 1 – 6.
- [4] T. Fu, X. Yue, H. Wu, C. Fu, T. Zhu, X. Liu, L. Hu, P. Ying, J. He, X. Zhao, Enhanced thermoelectric performance of PbTe bulk materials with figure of merit  $ZT > 2$  by multi-functional alloying, *J Materomics*. 2 (2016) 141 – 149.
- [5] J.P. Heremans, V. Jovovic, E.S. Toberer, A. Saramat, K. Kurosaki, A. Charoenphakdee, S. Yamanaka, G.J. Snyder, Enhancement of thermoelectric efficiency in PbTe by distortion of the electronic density of states, *Science*. 321 (2008) 554 – 557.
- [6] B. Poudel, Q. Hao, Y. Ma, Y. Lan, A. Minnich, B. Yu, X. Yan, D. Wang, A. Muto, D. Vashaee, X. Chen, J. Liu, M. Dresselhaus, G. Chen, Z. Ren, High-thermoelectric performance of nanostructured bismuth antimony telluride bulk alloys, *Science*. 320 (2008) 634 – 638.
- [7] W. Xie, X. Tang, Y. Yan, Q. Zhang, T.M. Tritt, Unique nanostructures and enhanced thermoelectric performance of melt-spun BiSbTe alloys, *Appl. Phys. Lett.* 94 (2009) 102111.
- [8] I. Terasaki, Large thermoelectric power in  $\text{NaCo}_2\text{O}_4$  single crystals, *Physical review b*, 56(20) (1997) R12685 – R12687.
- [9] I. Terasaki, Proceedings of the 18th International Conference on Thermoelectrics International Thermoelectric Society, 1999, pp. 569.
- [10] Y. Masuda, D. Nagahama, H. Itahara, T. Tani, W. S. Seo and K. Koumoto, Thermoelectric performance of Bi- and Na-substituted  $\text{Ca}_3\text{Co}_4\text{O}_9$  improved through ceramic texturing, *J. Mater. Chem.* 13(5) (2003) 1094 – 1099.
- [11] Gaojie Xu, R. Funahashi, M. Shikano, Q. Pu, Biao Liu, High temperature transport properties of  $\text{Ca}_{3-x}\text{Na}_x\text{Co}_4\text{O}_9$  system, *Solid State Commun.* 124(3) (2002) 73 – 76.
- [12] K. Park, K.Y. Ko, H -C. Kwon, S. Nahm, Improvement in thermoelectric properties of  $\text{CuAlO}_2$  by adding  $\text{Fe}_2\text{O}_3$ , *J. Alloys Compd.* 437 (2007) 1 – 6.
- [13] C. Liu, D.T. Morelli, Thermoelectric properties of hot-pressed and PECS-Sintered Magnesium doped copper aluminum oxide, *J. Electron. Mater.* 40 (2011) 678 – 681.
- [14] A.N. Banerjee, R. Maity, P.K. Ghosh, K.K. Chattopadhyay, Thermoelectric properties and electrical characteristics of sputter-deposited p- $\text{CuAlO}_2$  thin films, *Thin Solid Films*. 474 (2005) 261 – 266.
- [15] Abanti Nag, V. Shubha, Oxide Thermoelectric Materials: A Structure–Property Relationship, *J. Electron. Mater.* 43(4) (2014) 962 – 977.
- [16] H. Liu, X. Shi, F. Xu, L. Zhang, W. Zhang, L. Chen, Q. Li, C. Uher, T. Day, G. Snyder Jeffrey, G.J. Snyder, Copper ion liquid-like thermoelectrics, *Nat. Mater.* 11 (2012) 422 – 425.